

## PASSIVE FILMS ON STAINLESS STEELS AFTER GAMMA-RAY IRRADIATION, AS STUDIED BY ELECTROCHEMICAL IMPEDANCE SPECTROSCOPY

G. CAPOBIANCO, G. SANDONA', T. MONETTA\* and F. BELLUCCI\*

Dipartimento di Chimica Fisica, Università degli Studi di Padova, 2 via Loredan, 35131 Padova, Italy

\*Dipartimento di Ingegneria dei Materiali e della Produzione, Università degli Studi "Federico II",  
p.le Tecchio, 80125 Napoli, Italy

**Abstract**—The physical structure of the passive film formed by anodization on 446 stainless steel has been investigated by the Electrochemical Impedance Spectroscopy technique, before and after galvanostatic reduction in de-aerated borate/boric acid buffer solution or gamma-ray irradiation in bidistilled water. On the basis of appropriate models, the results obtained indicate that after galvanostatic reduction the passive film is composed of two layers, the external one showing a porous structure. After gamma-ray irradiation, the passive film seems thinner, with a homogeneous rather than porous structure.

### INTRODUCTION

DIFFERENT theories for passivation processes have been proposed through the years and classified<sup>1</sup> as: (i) metal modification theories, (ii) rate velocity theories, (iii) oxide film theories, and (iv) adsorption theories. The most current accepted theories belong to the latter two categories; in particular, the oxide film theories assume that a three-dimensional layer is formed at the metal-solution interface, retarding the dissolution of the underlying metallic substrate. Furthermore, the passive layer can be described as homogeneous<sup>2</sup> or heterogeneous;<sup>3-6</sup> in the first case, the passive current is provided by the ionic transport through the layer, while, in the second case, mass transport occurs through a thick porous layer. Models presented in the literature are, however, a simplification of the real system: surface and XPS analyses have undoubtedly shown that the composition of the passive layer changes in the direction perpendicular to the metal surface and also with the potential.<sup>7</sup>

In a recent paper,<sup>8</sup> the effect of gamma-ray irradiation on the passive film of anodized AISI 446 stainless steel samples in de-aerated bidistilled water has been reported, and compared with that obtained after a partial galvanostatic reduction of the anodized sample. The analysis of the XPS depth profiles of specimens before and after galvanostatic reduction or gamma-ray irradiation indicated that the passive layer was homogeneous and that, during the treatment, part of the oxide had been removed from the passive layer, with depletion of iron and a corresponding chromium enrichment, especially at the solution/oxide interface. Furthermore, the sputtering time required to reach the steel/oxide interface was less for the irradiated or galvanostatically reduced samples than for the anodized ones.

According to the difficulties to evaluate, from AES and XPS data, the depth of the oxide layer,<sup>9</sup> since the etching time is directly related to the density of the passive film, it is impossible to assert if the shorter etching time found for the irradiated and

the galvanostatically reduced specimens is due to the presence of a thinner layer or of a spongy film.

On the other hand, Electrochemical Impedance Spectroscopy (EIS) has proved to be a useful *in situ* technique for the understanding of the surface inhomogeneities on both microscopic or macroscopic scale,<sup>6</sup> with inhomogeneities that, in the latter case, can be due to adsorption phenomena, formation of porous or non-porous layers of different structure and/or composition, implying different electronic properties.

The aim of the present paper is thus the understanding of the physical structure of the passive layer formed on 446 stainless steel, before and after galvanostatic reduction or gamma-ray irradiation, by using the EIS technique, taking into account the phenomenological and physical approaches.

### EXPERIMENTAL METHOD

The electrode preparation, the electrolytic cell, the equipment and the techniques used, and details of the experimental procedures for the potentiostatic oxidation of samples, their galvanostatic reduction and gamma-ray irradiation, have been previously described.<sup>8</sup>

EIS experiments were performed in an equivolume mixture of 0.15 N  $\text{H}_3\text{BO}_3$  and  $\text{Na}_2\text{B}_4\text{O}_7 \cdot 10\text{H}_2\text{O}$  in de-aerated bidistilled water, at 25°C (pH = 8.70), where the bare sample shows a range of passivity between *ca* -0.6 and 0.4 V.<sup>8</sup> An EGG 273 potentiostat connected with a Solartron 1255 frequency response analyser was utilized, with a sinusoidal excitation wave of 10 mV amplitude applied to the specimen in the frequency range between 100 kHz and  $10^{-3}$  Hz. The maximum number of integration cycles on the transfer function analyser was set at 10 to strike a good balance between integration speed and accuracy.

Potential values are referred to the saturated calomel electrode (SCE).

### EXPERIMENTAL RESULTS AND DISCUSSION

#### 1. Phenomenological approach

This approach is based on the assumption that the impedance data obtained reflect the response of the entire passive film. A change in the composition and, consequently, in the properties of the passive film as a function of depth will therefore be 'seen' by the impedance method as a change in the 'average' value of the parameters of the passive film.

The results of the impedance measurements for the bare (B), anodically passivated (AP), galvanostatically reduced (GR) and gamma-ray irradiated ( $\gamma$ I) samples are presented in Fig. 1(a) and (b) as Bode and phase angle plots, respectively.

Frequency sweep curves for the samples in the passive state detected before and after reduction or irradiation exhibit a capacitive range that typically extends over several orders of magnitude. The Bode plot shows a linear, pseudo-capacitive response region at high and intermediate frequencies, and a deviation at lower frequencies for the bare and the irradiated samples. These results are confirmed by the phase angle plots.

The linear region on the Bode plot is characterized by the slope, intercept and phase angle. In particular, the phase angle at the low frequency regime is useful to characterize the resistive component, whereas the difference in magnitude of the phase angle in the pseudo-capacitive regime and at the lowest excitation frequencies is useful to illustrate the appearance of an additional resistive element in the equivalent circuit.

According to literature, it is convenient to compare the slope of the pseudo-

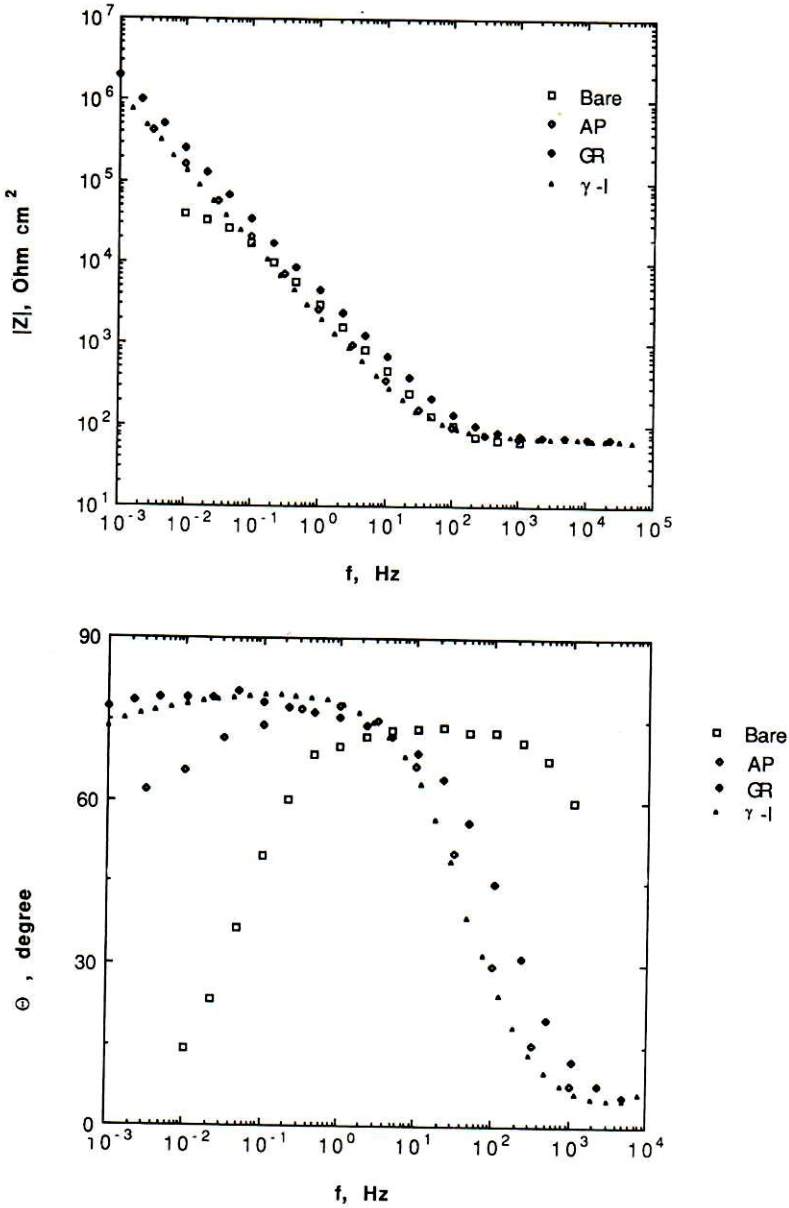


FIG. 1. Bode plot (a) and phase angle plot (b) of bare ( $\square$ ), anodically passivated ( $\diamond$ ), galvanostatically reduced ( $\blacklozenge$ ), and gamma-ray irradiated ( $\triangle$ ) 446 stainless steel samples, in de-aerated borate/boric acid buffer solution.

capacitive region, shown in Fig. 1(a), with those obtained with pure Fe and Cr in the same potential region.<sup>10</sup> For pure Fe, the slope decreases from  $-0.82$  at  $-0.7$  V, to  $-0.90$  at  $0.3$  V, indicating a more perfect capacitive behaviour as the potential is increased. The slope for pure Cr is already  $-0.91$  at  $-0.7$  V, and decreases to  $-0.95$  at  $-0.1$  V. In the passive region ( $-0.6$  to  $0.2$  V) for AP, GR and  $\gamma$ I samples slopes of  $-0.84$ ,  $-0.88$  and  $-0.91$  are observed, respectively; assuming that the slope

variation is prevalently due to the change of the chemical composition of the oxide film, rather than to structural effects or surface roughness, this should indicate a chromium enrichment of the passive layer, in agreement with the results of XPS analysis.<sup>8</sup>

The intercept of the plot  $\log Z$  vs  $\log f$  (where  $Z$  is the modulus of the impedance and  $f$  the frequency), corresponding to the  $Z$  value at 1 Hz, is equal to 3.64, 3.66 and 3.31 for the AP, GR and  $\gamma$ I samples, respectively.

For pure Fe and Cr, in the linear pseudo-capacitive regime the phase angles are fairly constant at 82–83° and 87°, respectively, over the potential region  $-0.4$  to  $0.7$  V. The AP, GR and  $\gamma$ I samples exhibit a maximum value of the phase angle equal to 77°, 80° and 79°, respectively.

As an indication of the appearance of a resistive component in the electrical equivalent circuit, it is useful to compare the values of  $\Delta\vartheta = \vartheta_{\max} - \vartheta_{f=10}^{-2}$ ; these values are equal to 11, 1 and 1 for the AP, GR and  $\gamma$ I samples; the corresponding value for the bare alloy is 60.

These results indicate that the passive film on the 446 alloy behaves like an imperfect capacitive element. The capacitive nature of the passive film is increased both after galvanostatic reduction and gamma-ray irradiation, and can be attributed to a chromium enrichment in the passive layer. The lower value of  $\log Z$  at 1 Hz observed after irradiation, together with the most pronounced capacitive behaviour, can be explained assuming a decrease of the thickness of the passive layer. The results for the GR sample can be explained in terms of a decrease of the passive layer thickness, with contemporaneous enrichment in Cr; in fact, the first effect leads to a decrease of the impedance, while the second leads to its increase. The experimental finding of  $\log Z$  obtained at 1 Hz indicates that for the GR sample these effects seem to compensate.

Although these results are consistent with the XPS analysis, they do not provide any further insight on the structure of the passive layer; hence, the physical model has been considered.

## 2. Physical model

Following Juttner,<sup>6</sup> a physical description of the passive film can be attempted, as first approximation, on the basis of a single or multilayer structure with 'passive' and 'active pit' models as schematically reported in Table 1. Theoretical transfer function for these models are reported elsewhere<sup>6</sup> and only the final comparing plots are shown in this paper. A dedicated software by Boukamp<sup>11</sup> was used to analyse and fit the experimental impedance data.

For the bare sample at the rest potential ( $-0.805$  V) the impedance spectrum can be described in terms of a solution resistance in series with a parallel combination of a pure charge transfer resistance and a double layer capacitance, with the overall transfer function corresponding to an ideal capacitive semicircle in the Nyquist plot. Deviations from this behaviour, attributable to inhomogeneities of the solid surface, can be described by using the Cole-Cole frequency dispersion formula<sup>12</sup> or by introducing a constant phase element (CPE), whose empirical admittance is of the type  $Y = Y_0 (j\omega)^n$ , where  $Y_0$  and  $n$  are constant. This CPE has proved of considerable value in data fitting, even if its physical meaning is not yet clear.<sup>13</sup> When the value of  $n$  is close to 1, the CPE behaves like a pure capacitor, whereas for  $n = 0.5$  the CPE is equivalent to a Warburg impedance.

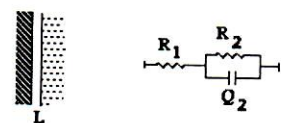
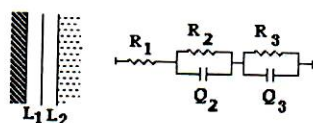
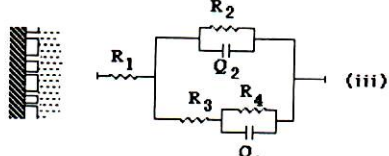
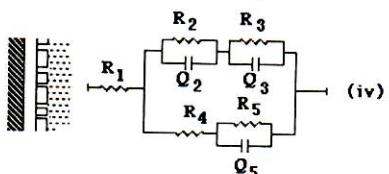
Experimental data relative to bare 446 alloy are well described by the above reported circuit with  $n = 0.85$ , suggesting that the electrochemical and corrosion behaviour of this sample can be properly described by a simple parallel RQ equivalent circuit.

To evaluate the most probable equivalent circuit capable of fitting the experimental data for the AP, GR and  $\gamma$ I samples, different models were considered (see Table 1): (i) a perfectly homogeneous single layer of thickness  $L$ ; (ii) perfectly homogeneous two layers of thickness  $L_1$  and  $L_2$ ; (iii) an imperfect single layer; (iv) an imperfect two layers. The analysis of the experimental data is based both on the mathematical fitting ( $\chi^2$  and residuals) and on the physical meaning of the parameters. Notwithstanding, it is not a simple task to discriminate among the different electrical circuits, owing to the lack of data at very low frequencies, even if the experiments were carried out up to  $10^{-3}$  Hz.

Fitting parameters evaluated for these models are reported in Table 1; a lower value of the parameter  $\chi^2$  indicates a better fitting of the experimental data by the transfer function of the equivalent circuit represented in the same Table. On the other hand, the phase angle plot is more sensitive to the appearance of resistive components, even when the contribution is still too small to cause a visible deviation from the linear behaviour of the Bode plot. Therefore, it is more convenient to compare the experimental and calculated data in terms of phase angle plot (Fig. 2a and b).

On this basis, the AP sample is well described by model (i), with  $R_1 = 71 \Omega$ ,  $R_2 = 1.3 \times 10^6 \Omega$ ,  $Q_2 = 7.3 \times 10^{-5}$ ,  $n_2 = 0.88$ . The physical structure of the passive layer of anodized 446 alloy is, therefore, composed of a single layer showing a resistive

TABLE 1. PROPOSED PHYSICAL MODELS, EQUIVALENT CIRCUITS AND  $\chi^2$  VALUES FOR THE INVESTIGATED SAMPLES.

	B	AP	GR	$\gamma$ -I
 (i)	$2.2 \times 10^{-2}$	0.12	$4 \times 10^{-3}$	$3 \times 10^{-3}$
 (ii)	1.63	0.2	$1.6 \times 10^{-4}$	$3 \times 10^{-2}$
 (iii)	1.81	0.2	$5.4 \times 10^{-3}$	$2.4 \times 10^{-2}$
 (iv)	$4 \times 10^{-2}$	0.76	$2.6 \times 10^{-4}$	$3.6 \times 10^{-2}$

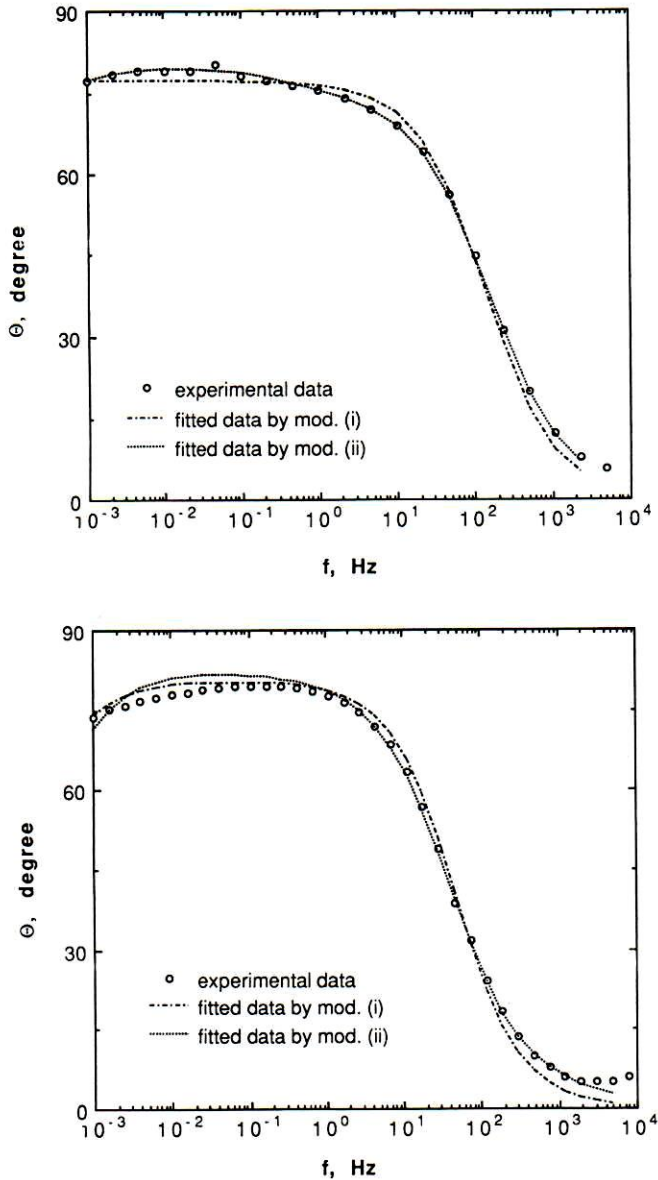


FIG. 2. Phase angle plots of passivated 446 stainless steel: experimental data detected (a) after galvanostatic reduction and (b) after gamma-ray irradiation (see Fig. 1), and optimum fitting results obtained using models (i) and (ii).

behaviour at low frequencies and a quasi-capacitive behaviour at intermediate frequencies.

Figure 2(a) shows the experimental EIS spectrum for the GR sample, compared with the theoretical fitting by using models (i) and (ii). On the basis of the values of  $\chi^2$  and residuals, the best fitting is obtained with model (ii) rather than model (i). Fitting parameters for both models are: (i)  $R_1 = 73 \Omega$ ,  $R_2 = 1.2 \times 10^{21} \Omega$ ,  $Q_2 =$

$4 \times 10^{-5}$ ,  $n_2 = 0.85$ ; (ii)  $R_1 = 67 \Omega$ ,  $R_2 = 812 \Omega$ ,  $Q_2 = 5 \times 10^{-5}$ ,  $n_2 = 0.63$ ,  $R_3 = 4.7 \times 10^7 \Omega$ ,  $Q_3 = 4.4 \times 10^{-5}$ ,  $n_3 = 0.90$ . After galvanostatic reduction, the passive layer behaves, according to model (i), like a quasi-capacitor or insulating film; according to model (ii) the passive film has instead a heterogeneous structure composed of an external, low resistance porous layer, as indicated by the value of  $n_2 = 0.63$ , and an inner, high resistive and quasi-capacitive layer.

Figure 2(b) shows the results for the  $\gamma$ I sample. Optimum fits are obtained with models (i) and (ii) also in this case, for the following parameters: (i)  $R_1 = 71 \Omega$ ,  $R_2 = 9 \times 10^6 \Omega$ ,  $Q_2 = 8.6 \times 10^{-5}$ ,  $n_2 = 0.89$ ; (ii)  $R_1 = 63 \Omega$ ,  $R_2 = 2.5 \times 10^{21} \Omega$ ,  $Q_2 = 5 \times 10^{-3}$ ,  $n_2 = 0.37$ ,  $R_3 = 5.6 \times 10^6 \Omega$ ,  $Q_3 = 9 \times 10^{-5}$ ,  $n_3 = 0.91$ . Model (i) appears to be more reasonable, due to the very low value of  $n_2$  obtained with model (ii). Model (iii) was not considered even if the corresponding  $\chi^2$  value is lower than for model (ii), due to the parameter values obtained ( $R_1 = 71 \Omega$ ,  $R_2 = 2.5 \times 10^{21} \Omega$ ,  $Q_2 = 8.9 \times 10^{-5}$ ,  $n_2 = 0.87$ ,  $R_3 = 2.5 \times 10^{-13} \Omega$ ,  $R_4 = 2.5 \times 10^{21} \Omega$ ,  $Q_4 = 4 \times 10^{-9}$ ,  $n_4 = -1$ ).

### CONCLUSIONS

The impedance measurements seem to suggest that the passive film formed by anodization on 446 stainless steel has a compact structure which is modified by galvanostatic reduction, leading to a film composed of two layers, the external one showing a coarse spongy-like physical structure, and by gamma-ray irradiation, leading to a thinner film with a better capacitive behaviour compared to that of the unirradiated sample. Electrochemical reduction appears, therefore, selective as far as the dissolution process at the interface is concerned.

*Acknowledgements*—This work has been supported by the Consiglio Nazionale delle Ricerche, Roma, Italy.

### REFERENCES

1. H. H. UHLIGH, *Proc. 4th Int. Symp. Passivity* (eds R. P. FRANKENTHAL and J. KRUGER), p. 1. The Electrochemical Soc., Princeton, New Jersey (1978).
2. C. Y. CHAO, L. F. LIN and D. D. MACDONALD, *J. electrochem. Soc.* **129**, 1974 (1982).
3. J. R. MACDONALD (ed.), *Impedance Spectroscopy*. Wiley, New York (1987).
4. J. R. PARK and D. D. MACDONALD, *Corros. Sci.* **23**, 295 (1983).
5. K. JUTTNER, W. J. LORENZ, M. W. KENDING and F. MANSFELD, *J. electrochem. Soc.* **135**, 332 (1988).
6. K. JUTTNER, *Electrochim. Acta* **35**, 1501 (1990).
7. N. SATO, *Proc. 4th Int. Symp. Passivity* (eds R. P. FRANKENTHAL and J. KRUGER), p. 29. The Electrochemical Soc., Princeton, New Jersey (1978).
8. G. CAPOBIANCO, G. PALMA, G. GRANOZZI and A. GLISENTI, *Corros. Sci.* **33**, 729 (1992).
9. S. MISCHLER, H. J. MATHIEU and D. LANDOLT, *Surf. Interface Anal.* **11**, 182 (1988).
10. M. J. KLOPPERS, *Electrochemistry of iron-chromium alloys*. PhD Thesis, MIT, Cambridge, MA (1991).
11. B. A. BOUKAMP, *Proc. 9th Eur. Congr. Corros.*, FU-252, Utrecht, The Netherlands (1989).
12. K. S. COLE and R. H. COLE, *J. chem. Phys.* **9**, 341 (1941).
13. J. R. MACDONALD, *J. electroanal. Chem.* **223**, 25 (1987).